Paper 185

Proceedings of the Eleventh International Conference
on Computational Structures Technology,
B.H.V. Topping, (Editor),
Civil-Comp Press, Stirlingshire, Scotland

A Hybrid Approach for Modelling Wave Propagation near Hollow Elastic Pipelines

P. Amado-Mendes, L. Godinho and A. Pereira
Research Centre on Building Sciences, CICC
Department of Civil Engineering, University of Coimbra, Portugal

Abstract

Underwater acoustics problems have been analysed by a variety of analytical and numerical methods. In many cases, the wave propagation is simulated applying different methodologies to obtain the solution of the wave-equation. When fluid-solid interaction is modelled, some approaches come to be complex and computationally very demanding. In the present work, the simulation of sound waves scattered by hollow elastic pipelines is tackled by a hybrid numerical-analytical model. The hollow elastic structures are assumed to be fluid-filled and embedded in a water waveguide with a sedimentary (fluid-like) bottom. The proposed approach consists of performing the coupling of analytical solutions, derived both for wave propagation in the host waveguide and near the circular hollow pipelines. The meshless method of fundamental solutions is adopted for coupling the appropriate analytical solutions, leading to precise results and a compact description of the propagation medium, very proficient from the computational point of view.

Keywords: hybrid numerical model, method of fundamental solutions, analytical solutions, multiple fluid-filled elastic shells, fluid-solid interaction.

1 Introduction

The detection of buried objects in solid and fluid media has been an active research topic, making use of different approaches. Techniques based on wave propagation modelling have received particular interest from researchers, leading to the development of a broad variety of analytical and numerical models to simulate this propagation, and to an intense research on the interpretation of field results. In the case of underwater acoustics, reference works include the now classic book by Jensen et al [1], which describes a number of formulations that can be used in both shallow water and deep water scattering problems.

In this paper, the authors focus on the scattering of waves in underwater configurations, for which different methods have been used in the past, ranging from the analytical methods presented by Pao and Mow [2], for studying wave diffraction near cylindrical circular inclusions, to purely numerical methods, such as finite difference (e.g. Stephens [3]) and finite elements techniques (e.g. Marfurt [4], Zampolli et al [5]), combined with transmitting boundaries.

The use of specific Green´s functions that account for part of the boundaries of the analysis domain has been an important strategy when dealing with boundary element methods, since they may allow for smaller discretization schemes, leading to lower computational effort, and therefore many researchers have focused their attention in their development. Relevant examples are the works of Tadeu and Kausel [6] and of Tadeu and António [7], who proposed 2.5D Greens´s functions for acoustic and elastic wave propagation in layered media, built as a superposition of the effects of plane waves with different inclinations; these functions have, in fact, been extensively used in subsequent works. António et al. [8] developed a Boundary Element formulation incorporating Green's functions to describe 2.5 D wave propagation for the case of a waveguide with an elastic bottom, and used them to study the scattering of waves by a buried or submerged object.

Recently, meshless methods have also been used for the study of underwater sound scattering in different types of environments. Different meshless methods are described in the literature, but in the present work we focus our attention on the Method of Fundamental Solutions (MFS) (e.g. Golberg and Chen [9]). An example of the application of this strategy to underwater acoustics can be found in the recent work by Costa et al [10], making use of the MFS together with fundamental solutions for a flat waveguide and for a perfect wedge.

The scattering by a submerged object located within a fluid medium has also been investigated by researchers, and works describing the scattering features of submerged circular cylindrical elastic shell structures have also been published. The wave scattering by submerged elastic circular cylindrical shells, filled with air, struck by plane harmonic acoustic waves was analyzed by Veksler et al. [11]. More recently, Godinho et al [12] described an analytical solution for the scattering of such structures buried in an homogeneous fluid medium. Later, the same authors [13] used a BEM formulation to analyze the effect of a construction defect in the vibration of such structures. However, it is important to note that this BEM formulation degenerates whenever the thickness of the structure is very small, and therefore alternative methods should be used.

In the present work, the authors address the case in which a regular circular shell structure is buried within a fluid seabed, under a water-filled flat waveguide. The approach proposed here is based on a hybrid approach which incorporates the analytical solutions described in [12] for the submerged circular shell structures, together with the analytical solution known for a waveguide with a fluid bottom (using the methodology proposed in [7]). The coupling of these solutions is performed in the fluid medium that describes the bottom by using the MFS and defining a virtual coupling boundary around the shell structure, along which the continuity of pressures and normal displacements is imposed.

Firstly, the governing equations of the problem are described in the frequency domain; then, the frequency domain multi-region MFS strategy for the coupling of the waveguide with the solid shells is formulated, followed by a brief description of the analytical solutions to be adopted for the submerged shell structures and for the waveguide with a fluid bottom. Afterwards, the procedure for calculating time responses from the computed frequency-domain results is referred; and, finally, a numerical simulation is presented, illustrating the applicability of the model to a realistic configuration.

2 Governing differential equations

Within the scope of this work, the 2D scattering of waves by cylindrical shell structures embedded within a fluid medium is analyzed. Thus, the governing equations of the problem correspond to the vectorial and scalar wave equations, respectively for the solid and for the fluid regions of the analysis domain.

Considering a homogeneous, linear isotropic elastic domain with mass density ρ_s, shear wave velocity β_s and compressional wave velocity α_s, the propagation of elastic waves can be described by vectorial wave equation

$$\alpha_s^{\,2}\,(\nabla\nabla\cdot\underline{\mathbf{u}})-\beta_s^{\,2}\,\nabla\times\nabla\times\underline{\mathbf{u}}=-\omega^2\,\underline{\mathbf{u}} \tag{1}$$

where the vector $\underline{\mathbf{u}}$ represents the displacement, ω is the circular frequency and, for a two-dimensional problem, $\nabla=\partial/\partial x\,\hat{\mathrm{i}}+\partial/\partial y\,\hat{\mathrm{j}}$; $\hat{\mathrm{i}}$ and $\hat{\mathrm{j}}$ are the unit vectors along the x and y directions.

If the propagation medium is a fluid, with mass density ρ_f, the propagation is governed by the Helmholtz equation, which can be written as

$$\nabla^2 p+k_f^{\,2}\,p=0 \tag{2}$$

where p is the pressure and $k_f=\omega/\alpha_f$ is the wave number, with α_f being the speed of sound in the fluid medium; for this scalar equation, $\nabla^2=\partial^2/\partial x^2+\partial^2/\partial y^2$.

Within this fluid medium, the displacements can be defined as a function of the first spatial derivative of p, and are given by

$$u_x=-\frac{1}{\rho_f\omega^2}\frac{\partial p}{\partial x} \tag{3a}$$

$$u_y=-\frac{1}{\rho_f\omega^2}\frac{\partial p}{\partial y} \tag{3b}$$

3 Formulation of the coupled numerical-analytical model

Consider a fluid waveguide, with a fluid bottom simulating a sedimentary seabed.

Within this seabed, an arbitrary number of circular, shell structures, made of elastic materials, and filled with a fluid material are embedded. This configuration is illustrated in Figure 1. A hybrid analytical-numerical model based on the Method of Fundamental Solutions (MFS) is proposed in this paper to calculate the pressure field within the waveguide generated by an acoustic source, placed at $\mathbf{x}_0$, in the presence of such configurations. For this purpose, consider that, in the presence of NR shell structures, the problem is divided in $NR+1$ subregions, one of them being the outer region, incorporating both the waveguide and the fluid bottom, and each of the NR subregions is defined around the shell structure, being limited by an interface around each structure, that corresponds to the coupling boundary interface. Outside this coupling boundary virtual sources are distributed for the internal region while inside the same interface virtual sources are placed for the outer region.

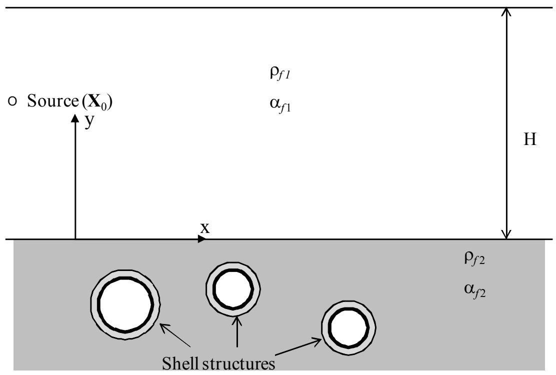

Figure 1: Generic representation of the problem to be solved, with fluid-filled elastic shell structures embedded in a bottom fluid halfspace below a waveguide.

When the fundamental solutions are known for each of the defined subregions, it is possible to establish a coupled model, which accounts for the full interaction between the involved fluids and the solids that compose the shell structures, by just establishing the continuity of pressures and displacements along the boundaries connecting the subregions. Using the MFS, the acoustic field in the outer subregion, containing the waveguide, can be defined by considering a number of virtual sources, $\sum_{j=1}^{NR} NVS_j$, placed within the remaining subregions, and combining their effects in a linear manner as

$$p(\mathbf{x}) = \sum_{j=1}^{NR} \sum_{l=1}^{NVS_j} a_{j,l} G^{waveguide}(\mathbf{x}, \mathbf{x}_{j,l}^{vs}) + G^{waveguide}(\mathbf{x}, \mathbf{x}_0), \tag{4a}$$

while for a receiver placed within fluid of the j th inner subregion we have

$$p(\mathbf{x}) = \sum_{l=1}^{NVS_j} a_{j,l} G^{shell}(\mathbf{x}, \mathbf{x}_{j,l}^{vs}), \tag{4b}$$

where $\mathbf{x}$ represents a point of coordinates (x, y), $\mathbf{x}_0$ is the position of the real source illuminating the system, $\mathbf{x}_{j,l}^{vs}$ is the position of each of the NVS_j virtual sources placed within subregion j, $G^{waveguide}(\mathbf{x},\mathbf{x}_0)$ is the fundamental solution for the waveguide with fluid bottom at a point $\mathbf{x}$ originated by a source positioned at $\mathbf{x}_0$; $G^{shell}(\mathbf{x},\mathbf{x}_0)$ is the fundamental solution for each interior subregion, incorporating the full interaction between the shell structures and the outer and inner fluids; the coefficients $a_{j,l}$ are, "a-priori", unknown and must be determined by establishing a system of equations, enforcing the continuity of pressures and displacements along each of the NR boundaries separating the outer subregion from each internal subregion.

Assuming that the boundary conditions are enforced at NVS_j collocation points along the kth coupling interface, the continuity equations on the mth collocation point $\mathbf{x}_m^{c,k}$ of that boundary can be written as

$$\sum_{j=1}^{NR}\sum_{l=1}^{NVS_j} a_{j,l} G^{waveguide}(\mathbf{x}_m^{c,k},\mathbf{x}_{j,l}^{vs}) + G^{waveguide}(\mathbf{x}_m^{c,k},\mathbf{x}_0) = \sum_{l=1}^{NVS_k} b_{k,l} G^{shell}(\mathbf{x}_m^{c,k},\mathbf{x}_{k,l}^{vs\_she} \tag{5a}$$

$$\begin{aligned}\sum_{j=1}^{NR}\sum_{l=1}^{NVS_j} a_{j,l}\frac{\partial}{\partial \vec{n}} G^{waveguide}(\mathbf{x}_m^{c,k},\mathbf{x}_{j,l}^{vs}) + \frac{\partial}{\partial \vec{n}} G^{waveguide}(\mathbf{x}_m^{c,k},\mathbf{x}_0) = \\ = \sum_{l=1}^{NVS_k} b_{k,l}\frac{\partial}{\partial \vec{n}} G^{shell}(\mathbf{x}_m^{c,k},\mathbf{x}_{k,l}^{vs\_shell})\end{aligned} \tag{5b}$$

where the coefficients $b_{k,l}$ are, "a-priori", unknown amplitudes of the fundamental solution for the region containing the shell structure.

A $N\times N$ linear system of equations, with $N = 2\times\sum_{j=1}^{NR} NVS_j$, can then be built. Once this system of equations is solved, one may obtain the pressure at any internal point by applying equations (4).

An important point that should be highlighted concerning this formulation is that the coupling between subregions is enforced in fluid-fluid interfaces, at some distance from the interfaces with the solid media that constitutes the shell structures. This strategy allows the coupling to be performed in a region with smooth variations of the pressure, which greatly improves the performance of the MFS. Additionally, since the interface between subregions is virtual, it can assume a smooth shape, such as that of a circle, which has been demonstrated in previous works that leads to very accurate results [14]. Finally, if the fundamental solutions are computed analytically within each subregion, a further step can be given towards obtaining high accuracy. In what follows, these fundamental solutions are briefly introduced.

3.1 Analytical model for a fluid waveguide with a fluid bottom

The Green's function for a flat fluid waveguide bounded bellow by a fluid halfspace (simulating a seabed) and above by a free surface can be obtained using the definition of displacement potentials, performing the decomposition of the wave field in terms of plane waves. These solutions are known for layered systems, and can be derived following the methodology presented by Tadeu et al [6, 7]. In this technique, the solutions can be expressed as the sum of the source terms equal to those in full space and of surface terms generated at the free surface and at the interface between the waveguide and the fluid halfspace, as depicted in Figure 2.

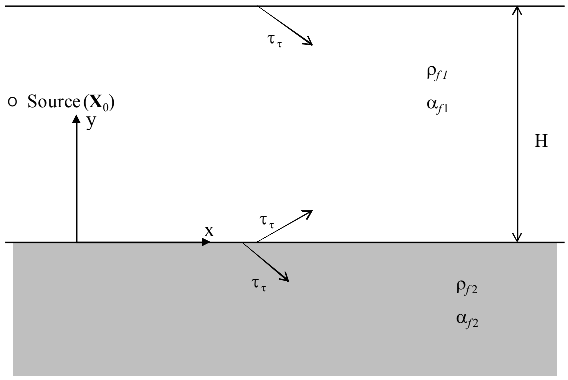

Figure 2: System with a fluid waveguide over a fluid seabed.

The Green's function at point $\mathbf{x}$, for an infinite homogeneous fluid medium, when a pressure load is applied at $\mathbf{x}_0$, with coordinates (x_0, y_0), can be obtained by derivation of a pressure potential for an infinite fluid space, expressed as a superposition of plane waves by means of a discrete wavenumber representation, leading to

$$G^{full}(\mathbf{x},\mathbf{x}_0) = -\frac{\mathrm{i}}{2L_x}\sum_{n=-N}^{n=+N}\left(\frac{E_{f1}}{\nu_n^{f1}}\right)E_d = -\frac{\mathrm{i}}{4}\mathrm{H}_0\left(k_{\alpha 1} r\right), \tag{6}$$

where $E_{f1} = \mathrm{e}^{-\mathrm{i}\nu_n^{f1}|y-y_0|}$, $E_d = \mathrm{e}^{-\mathrm{i}k_n(x-x_0)}$, $\nu_n^{f1} = \sqrt{k_{\alpha 1}^2 - k_n^2}$ with $\mathrm{Im}\left(\nu_n^{f1}\right) \le 0$, $k_{\alpha 1} = \omega/\alpha_{f1}$, $r = \sqrt{(x-x_0)^2 + (y-y_0)^2}$ and $H_n(\ldots)$ represent Hankel functions of the second kind and order n. A space interval along the x direction of L_x is assumed between a set of virtual plane sources distributed along that direction. In order to avoid the influence of neighboring fictitious sources in the response, complex frequencies of the form $\omega_c = \omega - \mathrm{i}\times\xi$ have been used [7].

The Green's functions for the fluid layer are given by the sum of the source terms and the surface terms originated in both interfaces. When a pressure source excites the waveguide, that procedure leads to the following expressions for the pressure field in the system:

$$G^{waveguide}\left(\mathbf{x},\mathbf{x}_0\right) = G^{full}\left(\mathbf{x},\mathbf{x}_0\right) - \frac{\mathrm{i}}{2L_x}\sum_{n=-N}^{n=+N}\left(\frac{E_f^1}{\nu_n^{f1}}B_n^1 + \frac{E_f^2}{\nu_n^{f1}}B_n^2\right)E_d \tag{7a}$$

$$G^{waveguide}\left(\mathbf{x},\mathbf{x}_0\right) = -\frac{\mathrm{i}}{2L_x}\sum_{n=-N}^{n=+N}\left(\frac{E_f^3}{\nu_n^{f2}}B_n^3\right)E_d \tag{7b}$$

with $E_f^1 = \mathrm{e}^{-\mathrm{i}\nu_n^{f1}|y-H|}$, $E_f^2 = \mathrm{e}^{-\mathrm{i}\nu_n^{f1}|y|}$, $E_f^3 = \mathrm{e}^{-\mathrm{i}\nu_n^{f2}|y|}$, $\nu_n^{f2} = \sqrt{k_{\alpha 2}^2 - k_n^2}$ with $\mathrm{Im}\left(\nu_n^{f2}\right) \le 0$, and $k_{\alpha 2} = \omega/\alpha_{f2}$. B_n^1, B_n^2 and B_n^3 correspond to unknown coefficients that are determined after solving a system of equations, built with potentials so that the field, produced simultaneously by the source and the surface terms, should satisfy the appropriate boundary conditions at the interfaces.

3.2 Analytical model for a circular cylindrical shell embedded in a fluid medium

Consider a circular shell solid structure, defined by the internal and external radii r_A and r_B, respectively, and submerged in a homogenous fluid medium, as illustrated in Figure 3. A harmonic dilatational source, placed in the exterior fluid medium, is assumed to illuminate the system, generating waves that hit the surface of the submerged structure. Part of the incident energy is then reflected back to the exterior fluid medium, with the rest being transmitted into the solid material, where they propagate as body and guided waves. These waves continue to propagate and may eventually hit the inner surface of the structure, where similar phenomena occur. The wavefield generated in the exterior fluid medium (Fluid 2) depends both on the incident pressure waves and on those coming from the external surface of the shell. The analytical solution for the scattering of such structures has been described by Godinho et al [12, 13], where the displacement potentials were defined, the adequate boundary conditions were established and the final equation system was presented.

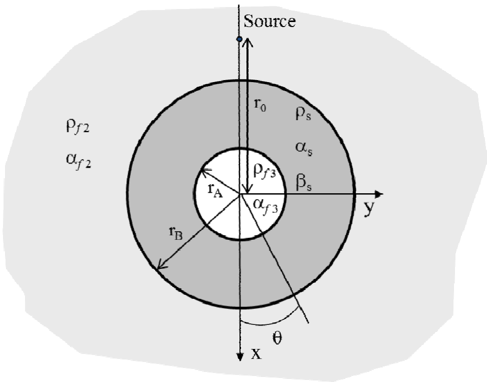

Figure 3: Circular cylindrical shell structure submerged in a fluid medium.

For the outer fluid, the pressure field at point (x,y) can be written as

$$G^{shell}(\mathbf{x},\mathbf{x}_0) = -\frac{\mathrm{i}}{4}\mathrm{H}_0(k_{\alpha 2}\sqrt{(x-x_0)^2+(y-y_0)^2}) + \sum_{n=0}^{N} A_n^1 \mathrm{H}_n(k_{\alpha 2} r)\cos(n\theta) \tag{8}$$

with A_n^1 representing one of the terms A_n^j $\left(j=1,6\right)$ to be obtained by solving the referred system of equations.

The displacement field can then be determined by applying equation (3).

4 Time domain responses

The pressure responses in the spatial-temporal domain are obtained by modeling a Ricker wavelet, whose Fourier transform is

$$U\left(\omega\right)=A\left[2\pi^{1/2}t_o\mathrm{e}^{-\mathrm{i}\omega t_s}\right]\Omega^2\mathrm{e}^{-\Omega^2} \tag{9}$$

in which $\Omega=\omega t_o/2$; A is the amplitude; t_s is the time when the maximum occurs and πt_o is the characteristic (dominant) period of the wavelet.

This signal form was chosen as it decays rapidly, both in time and frequency, thus reducing computational effort and allowing easier interpretation of the computed time series and synthetic waveforms.

Complex frequencies of the form $\omega_c=\omega-\mathrm{i}\zeta$, with $\zeta=0.7\Delta\omega$, were used because the influence of the neighboring fictitious sources is reduced and the aliasing phenomena are avoided. In the time domain, this shift is later taken into account by applying an exponential window $\mathrm{e}^{\xi t}$ to the response [15].

5 Model verification

The verification of the proposed coupling methodology was performed by comparing its results with those obtained using other techniques in different situations. Since no analytical solution is known for the complete problem addressed in the present work, this verification was performed against other numerical methods, namely the Boundary Element Method (BEM). In the comparisons that were carried out, along the full set of frequencies analyzed, the results matched perfectly. However, in order to better understand the behavior of this hybrid method, an additional numerical study was performed concerning the variability of its results with the number of collocation points and with the position of the virtual sources. For this purpose, consider the system represented in Figure 4, in which two buried elastic shell structures are embedded within a seabed with different properties from the waveguide. Consider the case of an acoustic water waveguide, allowing a propagation velocity of $1500\ \mathrm{m/s}$, and exhibiting a density of $1000\ \mathrm{kg/m^3}$, with a depth of $20.0\ \mathrm{m}$. Bellow this waveguide, a fluid seabed is considered, allowing sound to travel at $2100\ \mathrm{m/s}$, and exhibiting a density of $1800\ \mathrm{kg/m^3}$. The two circular structures have an external radius of $1.0\ \mathrm{m}$ and an internal radius of $0.5\ \mathrm{m}$, and are positioned at $x=3.0\ \mathrm{m}$ and $y=-4.0\ \mathrm{m}$ and at $x=6.0\ \mathrm{m}$ and $y=-4.0\ \mathrm{m}$. The shell structure is made of an elastic material with a density of $1400\ \mathrm{kg/m^3}$, and allowing propagation velocities for the P and S waves of $2182.2\ \mathrm{m/s}$ and of

1336.6 m/s, respectively. To couple the waveguide with the two structures, two virtual interfaces with a radius of 1.2 m are defined.

The response has been calculated for a frequency of 2000 Hz, at a receiver placed at $x = 5.0$ m and $y = -2.0$ m, using different numbers of collocation points and positioning the virtual sources at different distances from the virtual interfaces between the shell regions and the waveguide region.

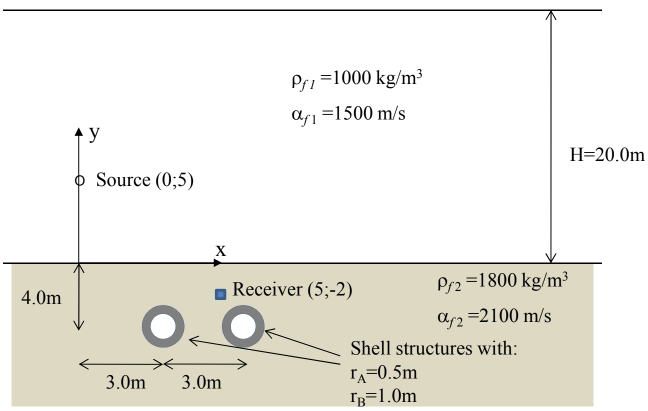

Figure 4: Schematic representation of the system with two buried shell structures.

Figure 5 presents the results at that receiver, calculated for 30 collocation points, when the distance between the virtual sources and the interface (D) assumes different values. In that figure, the relation D / R is used to define the distance as a function of the radius of the coupling interface (R). As can be observed, the response is stable as long as the virtual sources are not very close to the interface. In fact, for that case, a singularity of the fundamental solution occurs very close to the boundary, degrading the quality of the result. When D / R is 0.3 or larger, the variation of the response is very small, and indicates a good behavior of the coupling strategy.

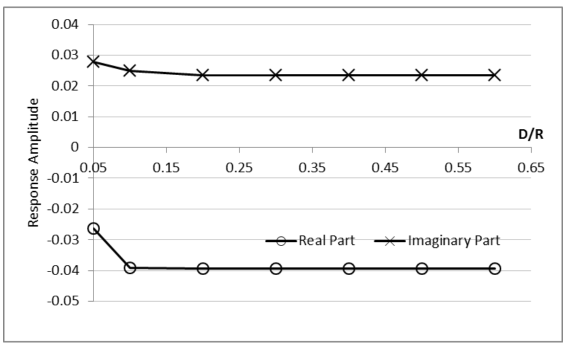

Figure 5: Response at the field point ($x = 5.0$ m and $y = -2.0$ m) when 30 collocation points are used and for different positions of the virtual sources.

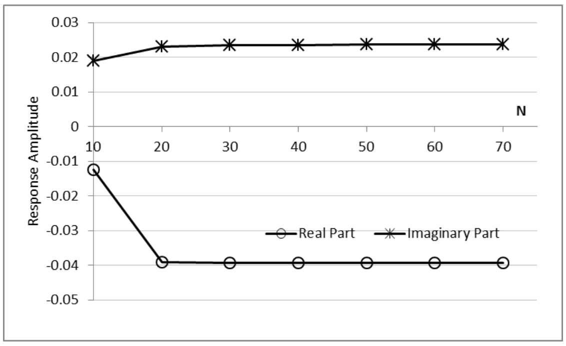

Figure 6: Response at the field point ($x = 5.0$ m and $y = -2.0$ m) when different numbers of collocation points are used and the distance from the virtual sources to the interface is 0.4 times the radius of the fictitious interface.

6 Numerical example

In order to illustrate the applicability of the proposed numerical approach, consider now a fluid waveguide, 20.0 m deep, with a sedimentary seabed, as displayed in Figure 7. Assume that the fluid inside the waveguide is water, with a density $\rho_{f1} = 1000.0$ kg/m^3 and allowing a dilatational wave velocity $\alpha_{f1} = 1500.0$ m/s. The sedimentary seabed is modeled with a density $\rho_{f2} = 1800.0$ kg/m^3 and permits the propagation of dilatational waves with a velocity $\alpha_{f2} = 2100.0$ m/s, corresponding to a scenario where the properties of the seabed do not differ significantly from those of the fluid medium.

Within the seabed, consider the presence of two identical circular shell structures with external and internal radii $r_B = 1.0$m and $r_A = 0.95$m, respectively, made of an elastic material with density $\rho_s = 7850.0$ kg/m^3, and allowing a dilatational wave velocity $\alpha_s = 6009.0$ m/s and a shear wave velocity $\beta_s = 3212.0$ m/s; these structures are filled with a fluid material with the same properties as water. This system is excited by a cylindrical pressure source placed near the bottom of the waveguide at $x = -10.0$ m and $y = 2.0$ m.

To simulate this problem, two virtual circular interfaces with a radius of 1.2 m are defined to account for the two subdomains containing the buried structures. Each of those interfaces is defined using 35 collocation points, and two sets of virtual sources are positioned at a distance of 0.4 times the radius of the virtual interface. Calculations are then performed over a frequency range between 20.0 Hz and 2560.0 Hz, assuming a frequency step of 20.0 Hz; for the purpose of calculating time responses, the defined increment allows a total analysis time of $T = 50.0$ ms. Time domain signals are computed by means of an inverse Fourier transform, using the methodology described earlier.

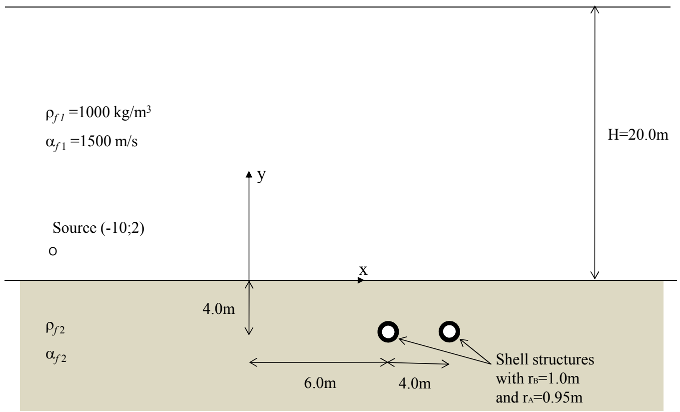

Figure 7: Geometry defined for the numerical example.

The pressure field in the waveguide was computed over a grid of receivers, equally spaced at $\Delta x = 0.5$ m, $\Delta y = 0.5$ m, placed between: $x = 0.0$ m and $x = 25.0$ m; $y = 0.0$ m and $y = 20.0$ m. A set of snapshots representing the pressure wave field over the grid of receivers is presented. Figure 8 displays snapshots of the pressure response, for different time instants, over the grid of receivers placed in the waveguide, generated by a source emitting a Ricker pulse with a characteristic frequency $f_k = 400$ Hz. A grayscale is used to represent the amplitudes of the waves arriving at the receivers, with lighter colors corresponding to higher values and darker colors representing lower values. In the first column of Figure 8 the reference responses were computed without shell structures buried in the sedimentary seabed.

At time $t = 0.0$ ms, the load creates a cylindrical pressure wave that propagates away from it. In Figure 8a1, corresponding to $t = 14.6$ ms, this incident pulse is visible (identified as P1), followed by a first reflection from the bottom of the waveguide (identified as P2). At receivers placed near the ground, a third reflection may also be identified, which is related to the head wave generated in the surface of the seabed (identified as P3). This wave is originated at the interface between the two media, and travels along this interface with the velocity of the faster medium, which is the seabed, with $\alpha_{f2} = 2100.0$ m/s; therefore it appears in the plot at receivers placed farther from the source. As time increases, it is possible to identify the reflections generated at the free surface (identified as P4), with inverted polarity (see Figure 8b1). For subsequent instants, a sequence of pulses originated by multiple reflections in the surface and bottom of the waveguide can be identified (see Figure 8c1 and 8d1). These reflections tend to loose energy as time increases, with part of the energy being transmitted to the seabed, and a stationary field is generated inside the waveguide by these waves, which travel up and down between the surfaces of the channel, and tend to become flat as time increases.

When the two shell structures are buried in the seabed, a different wave pattern inside the waveguide may be originated. In order to try to detect the presence of these structures, snapshots of the sound propagation within the waveguide were captured (see second column of Figure 8).

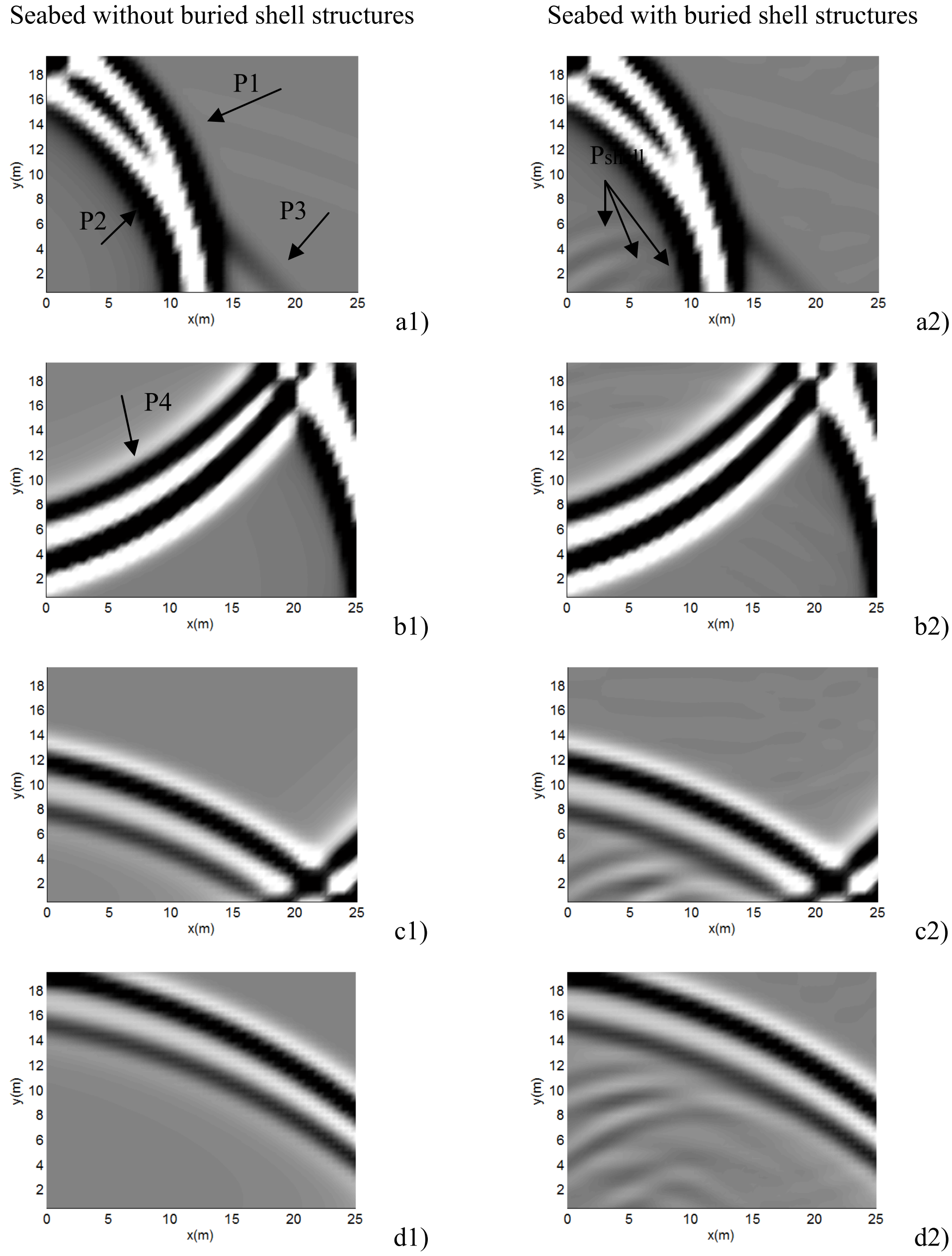

Figure 8: Snapshots displaying the pressure wave fields over the grid of receivers placed in the waveguide with a seabed (left column, without buried shell structures; right column, with buried shell structures): a) $t = 14.6$ ms ; b) $t = 24.4$ ms ; c) $t = 34.2$ ms ; d) $t = 39.1$ ms .

A set of additional pulses appear in the response (labeled as Pshell), which refer to reflections originated by the presence of the shell structures. These reflections, can further be identified in the snapshots corresponding to subsequent instants (see Figures 8b2-d2), although displaying smaller amplitudes, due to the contrast between media, which tends to hinder energy exchanges. For later instants, the responses display multiple pulses, related not only to reflections of waves generated in the waveguide, but also to several reflections originated at the shell structures, at the top and at the bottom of the waveguide. It is also interesting to note that the reflection pattern originated at the buried structures is quite complex, revealing multiple reverberation effects that occur not only between the structures and the sea bottom, but also within the structures themselves and within the fluid that fills their interior.

7 Conclusions

In this paper, the coupling between different analytical solutions using the MFS is proposed to study the problem of scattering of acoustic waves in a waveguide in the presence of buried structures. The scattering structure is assumed to be buried in the fluid seabed bellow a water waveguide, and consists of circular elastic shells filled with a fluid that may have different properties from the host medium. The proposed strategy was formulated and implemented, and was found to provide good results when compared with alternative numerical modelling techniques. Since it performs the coupling between closed-form solutions, the method provides accurate results, while allowing a compact and simple model description. One major advantage of the proposed model is that it allows the simulation of very thin solid structures, without the problems usually associated with thin bodies when using alternative methods. A numerical example was presented to illustrate the applicability of the proposed methodology, revealing interesting signal features of the modified wave field observed in the waveguide as a consequence of the presence of the hollow pipelines embedded in the bottom stratus.

Acknowledgments

The authors acknowledge the “Instituto de Investigação e Desenvolvimento Tecnológico em Ciências da Construção – ITeCons”, for the support provided during the preparation of this study.

References

[1] F.B. Jensen, W.A. Kuperman, M.B. Porter, and H. Schmidt, *Computational Ocean Acoustics*, American Institute of Physics, Woodbury, NY, 2000.

[2] Y.H. Pao, C.C. Mow, *Diffraction of Elastic Waves and Dynamic Stress Concentrations*, Crane and Russak, 1973.

[3] R.A. Stephens, “A review of finite difference methods for seismo-acoustic problems at the seafloor”, Rev. Geophys., 26, 445-458, 1988.

[4] K.J. Marfurt, “Accuracy of finite-difference and finite-element modeling of the scalar and elastic wave equations”, Geophysics, 49, 533-549, 1984.

[5] M. Zampolli, A. Tesei, F.B. Jensen, N. Malm, J.B. Blottman, “A computationally efficient finite element model with perfectly matched layers applied to scattering from axially symmetric objects”, J. Acoust. Soc. Am., 122(3), 1472-1485, 2007.

[6] A. Tadeu E. Kausel, “Green’s functions for two-and-a half dimensional elastodynamic problems”, Journal of Engineering Mechanics ASCE, 126 (10), 1093-1097, 2000.
[7] A. Tadeu J. António, “2.5D Green functions for elastodynamic problems in layered acoustic and elastic formations”, Journal of Computer Modelling in Engineering and Sciences CMES, 477-496, 2001.
[8] J. António, A. Tadeu, L. Godinho, “2.5D scattering of waves by rigid inclusions buried under a fluid channel via BEM”, European Journal of Mechanics /A-Solids, 24(6), 957–973, 2005.
[9] M.A. Golberg, C.S. Chen, The method of fundamental solutions for potential, Helmholtz and diffusion problems, In: *Boundary Integral Methods: Numerical and Mathematical Aspects*, M.A. Golberg (editor), WIT Press & Computational Mechanics Publications, Boston, Southampton, 103-176, 1999.
[10] E.G.A. Costa, L. Godinho, J.A.F. Santiago, A. Pereira, C. Dors, “Efficient numerical models for the prediction of acoustic wave propagation in the vicinity of a wedge coastal region”, Engineering Analysis with Boundary Elements, 35, 855–867, 2011.
[11] N. Veksler, J. Izbicki, J. Conoir, “Bending a wave in the scattering by a circular cylindrical shell: its relation with the bending free modes”, J. Acoust. Soc. Am., 96 (1), 287–293, 1994.
[12] L. Godinho, A. Tadeu, F. Branco, “Dynamic analysis of submerged fluid-filled pipelines subjected to a point pressure load”, Journal of Sound and Vibration, 271(1-2), 257-277, 2004.
[13] L. Godinho, A. Tadeu, F. Branco, “Wave scattering by infinite ring shaped structures submerged in a fluid medium”, Journal of Wave Motion, 38(2), 131-149, 2003.
[14] L. Godinho, A. Tadeu, P.A. Mendes, “Wave propagation around thin structures using the MFS”, Computers, Materials and Continua (CMC), 5(2), 117-127, 2007.
[15] E. Kausel, J.M. Roesset, “Frequency domain analysis of undamped systems”, Journal of Engineering Mechanics ASCE, 118, 721-734, 1992.